Covalent Protein Inhibitors via Tyrosine Conjugation with Cyclic Imine Mannich Electrophiles

Sijie Wang[1], Marco Hadisurya[2], W. Andy Tao[2,3], Emily C. Dykhuizen[1,3], Casey J. Krusemark[1,3*]

[1]Department of Medicinal Chemistry and Molecular Pharmacology, Purdue University, West Lafayette, Indiana 47907, United States

[2]Department of Biochemistry, Purdue University, West Lafayette, Indiana 47907, United States

[3]Purdue Center for Cancer Research, West Lafayette, Indiana 47907, United States

ABSTRACT: Targeted covalent inhibitors (TCIs) have increased in popularity among drug candidates and chemical probes. Among current TCIs, the chemistry employed is largely limited to labeling cysteine and lysine side chains. Tyrosine is an attractive residue for TCIs due to its enrichment at protein-protein interfaces. Here, we investigate the utility of cyclic imine Mannich electrophiles as covalent warheads to specifically target a protein tyrosine adjacent to an inhibitor binding pocket. We characterized the intrinsic reaction rates of several cyclic imines to tyrosine and identified the iminolactone to be suitable for a covalent inhibitor (second order rate constant of 0.0029 M^{-1} s^{-1}). We appended the cyclic imine warheads to a CBX8 chromodomain inhibitor to label a non-conserved tyrosine, which markedly improves both the potency and selectivity of the inhibitor for CBX8 *in vitro* and in cells. These results indicate that Mannich electrophiles are promising and robust chemical warheads for tyrosine bioconjugation and covalent inhibitors

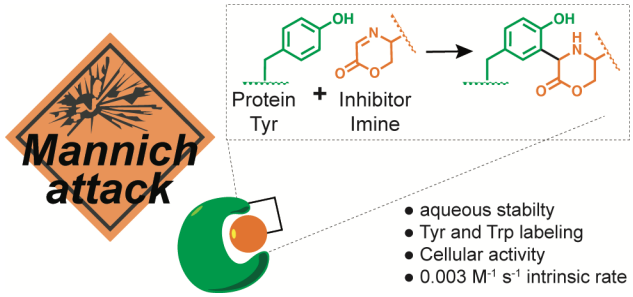

INTRODUCTION

The number and diversity of covalent inhibitors has increased dramatically in recent years. The majority are targeted covalent inhibitors (TCIs), which are rationally designed to bind to a protein target and then form a covalent bond. A TCI brings a reactive moiety (typically an electrophile of low reactivity) directly adjacent to an amino acid side chain, inducing a high effective concentration. This leads to a selective covalent conjugation to a proximal amino acid side chain to yield an inhibitor with irreversible occupancy.[1,2]

Covalent labeling has multiple advantages as a tool in probe and drug development.[3] Compared with noncovalent inhibitors, TCIs can provide increased selectivity, increased potency, and prolonged modulation of target function. Covalent conjugation has enabled inhibition of targets at PPIs that were previously thought to be undruggable.[4,5] PPI covalent inhibitors approved by FDA or in clinical trials have shown great promise in recent years.[6–14] Currently, suitable chemistry for covalent inhibitor conjugation is dominated by thiol-reactive electrophiles that react with cysteine side chains. Cysteines, however, are rare amino acids and are also poorly represented at PPIs.[5,15–17] Development of additional chemical warheads for targeting additional residues will further expand the utility of TCIs.[1,18]

Tyrosines are attractive targets due to their functions in non-covalent interactions including hydrogen bonding, cation-π or π-π interactions, and hydrophobic interactions.[19–21] While tyrosine is an amino acid of low abundance (3% of protein amino acids),[22] it is highly enriched at protein-protein interfaces (PPIs).[4,5] Specifically, tyrosines are enriched in the histone binding pockets of epigenetic regulator proteins containing bromodomains (BrDs) and chromodomains (ChDs).[23,24] Development of adequately selective and potent small-molecule inhibitors for chromodomains, in particular, has shown to be challenging.[25,26]

The chemistry for targeting tyrosine has largely been limited to sulfonyl fluorides and fluorosulfonates, which react with the phenolic oxygen as the nucleophile.[27,28] [29,30] However, these warheads are not selective for tyrosine and react with lysine, serine, threonine, and histidine.[21,29,31] In addition, they have limited hydrolytic stability, with sulfonyl fluorides displaying particular lability. Additional chemistries have been employed for modifying tyrosine in bioconjugation but have not been employed in ligand-directed chemistry in cells due to high reactivity or

poor stability. For example, thiazolinedione (TAD) reagents show rapid reactivity and Tyr/Trp selectivity under mild conditions but have poor aqueous stability and decompose to the isocyanate, which labels additional residues (e.g. Lys/Cys).[32,33] Similarly, aryl diazonium salts have seen utility in Tyr conjugation, but high reactivity and poor stability limits use in a TCI. [34–36]

In 2004, the Francis group reported a three-component Mannich reaction to selectively modify protein tyrosines and tryptophans via the Betti variant of the Mannich reaction.[37,44] The development of a two-component reaction by the Tanaka Lab using a pre-formed, cyclic imine (an iminolactam) improved stability against hydrolysis and increased reactivity to phenols over a broad pH range.[38] In this work, we utilize two-component Mannich chemistry for modification of Tyr side chains and creation of TCIs with *in vitro* and cellular efficacy. We first explore the intrinsic reactivity of various cyclic imine derivatives on amino acid mimetics, and then append optimal Mannich electrophiles to inhibitors of CBX chromodomains to create a highly selective CBX8 inhibitor through Tyr modification. The improved cellular efficacy and proteome-wide selectivity indicate that cyclic imines have excellent promise as chemo-selective warheads to label tyrosine or tryptophan.

RESULTS AND DISCUSSION

Reactions of cyclic imines with tyrosine. Several cyclic imines (5 mM) were incubated with a simple tyrosine analog N-acetyl-L-tyrosine methylamide (Ac-Tyr-NHMe) in PBS pH 7 at 37 °C (Table 1, Figure 1). The reactivity was quantitated by UV integration on HPLC with LC/MS confirmation of reaction product identity (Figure S1). Under these pseudo-first order reaction conditions, reaction half-lives and second-order rate constants were determined.

We observed similar reactivity of the cyclohexyliminolactam **1** to that previously reported by Tanaka et al using p-cresol.[38] The reaction half-life ($t_{1/2}$) of imine **1** was 8 ± 0.3 hours under these conditions with a second-order rate constant of 2.4 × 10^{-4} M^{-1} s^{-1} at 37 °C (Figure 1) and 1.5 × 10^{-4} M^{-1} s^{-1} at R.T. (Figure S2). The iminolactone **2** reacted faster with a $t_{1/2}$ = 40 mins and second-order rate constant of 2.9 × 10^{-3} M^{-1} s^{-1} at 37 °C (Figure 1). This reaction rate compares favorably to the range of intrinsic rates of acrylamide electrophiles to cysteine (1 x 10^{-2} to 1 x 10^{-4} M^{-1} s^{-1}), which are the most commonly used reactive groups in covalent drugs.[39] The ~10-fold increase in rate constant of **2** relative to **1** indicates the tunability of imine reactivity with adjacent electron withdrawing groups. Further increasing electron withdrawing properties using aromatic ester imine **3** did increase the rate of Mannich addition, but hydrolysis of the phenol ester was a competing reaction. While stable in water, we observed 70% hydrolysis of **3** in PBS pH 7 within an hour. Compound **4,** with the less reactive amide, (drawn as the analogous tautomer of 2-hydroxyquinoxaline in Table 1) was unreactive, which was anticipated due to aromaticity. We hypothesized N-alkylation with a propargyl group would increase the tautomeric preference towards the reactive imine; however, compound **5** was also unreactive. Since protonation of the imine can be rate-limiting in the Mannich reaction[40], we

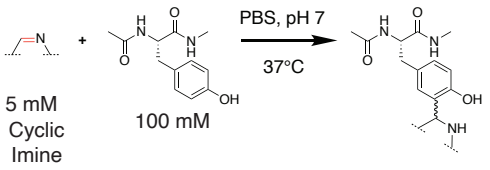

Compound	Reactivity ($t_{1/2}$)	Compound	Reactivity ($t_{1/2}$)
1 mixture of trans isomers	8 ± 0.3 hrs	**6** mixture of trans isomers	33 ± 3 hrs
2	40 ± 2 mins	**7**	30% conv. in 72 hours
3	30% conv. in 30 mins (competing hydrolysis)	**8**	No reactivity
4	No reactivity	**9**	5% conv. in 24 hours
5	No reactivity	**10**	No reactivity

Table 1. Reaction of cyclic imine Mannich electrophiles (5 mM) with *N*-acetyl-l-tyrosine methyl amide (100 mM) in PBS pH 7 at 37 °C. The reaction was monitored using LC/MS.

reasoned that an iminium may lead to enhanced reactivity, similar to recent work with a proline-selective Petasis reaction.[41] Iminium **6**, however, was less reactive than other imines ($t_{1/2}$~33 hours, Figure S2), presumably due to equilibrium favoring either the hydrate or the open, aldehyde forms[42]. Commercially available dihydro-beta-carbolines showed either very weak (compound **7**) or no reactivity (compound **8**). Other imines showed limited (compound **9**) or no (compound **10**) reactivity to tyrosine, as summarized in Table 1.

Reactivity of cyclic imines to additional amino acid mimetics. To assess the selectivity to other amino acids, we tested compounds mimicking amino acid side chain functional groups, including β-mercaptoethanol (cysteine), imidazole (histidine), isopropanol (serine/threonine), n-butylamine (lysine), propionic acid (aspartic acid/glutamic acid), 3-methyl indole (tryptophan), and N-ethyl pyrrole (pyrrole-lysine). We observed stable conjugates to **1** for β-mercaptoethanol, 3-methyl indole, and N-ethyl pyrrole by LC/MS analysis (Figure S3). Conjugation to thiols was expected based on previous reports.[38,43] While partially stable under LC/MS conditions, the *N,S*-thioaminal product was not stable under stronger acidic conditions (0.1 M HCl) and is readily reversible (see below).[43]

The tryptophan mimic, 3-methyl indole, reacts with **1** to form multiple products, likely a mixture of N-substitution and C2/C3- Mannich- or Pictet Spangler-type additions.[44–

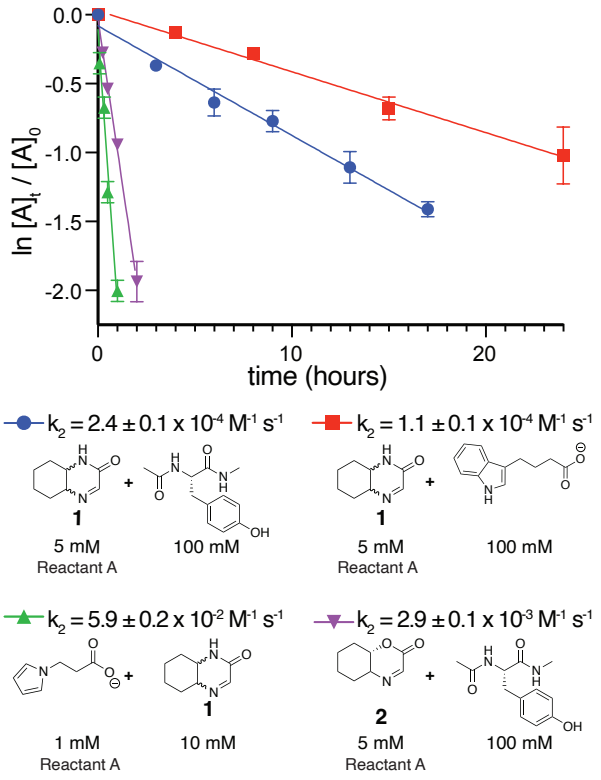

Figure 1. Second-order rate constants for select cyclic imines with aromatic nucleophiles. Reactions were conducted under pseudo first order conditions with an excess of one reactant, as indicated. The reduction in the concentration of the limiting reactant **A** was measured at various time points by HPLC analysis. Rates of imine **1** with N-Ac-Tyr-NMe, indole-3-butyric acid, and 1*H*-pyrrole-1-propionic acid and of imine **2** with N-Ac-Tyr-NMe were measured.

[46] (Figure S3). The poor aqueous solubility of 3-methyl indole made it challenging to obtain a rate constant and may explain conflicting results from a prior report that did not observe reactivity with imine **1**.[47] Using indole-3-butyrate as an alternative tryptophan mimic with enhanced solubility, we determined the rate constant (k_2 =1.1 × 10^{-4} M^{-1} s^{-1} at 37 °C) (Figure 1, Figure S1, S2), which was only 2-fold lower than the rate constant to tyrosine.

We also tested **1** with N-ethyl pyrrole as a mimic of pyrrolated lysine, a lesser-known posttranslational modification.[48,49] Pyrroles are particularly electron-rich aromatic groups that react rapidly in Mannich-type reactions. Previous work with N-pyrrolyl alanine derivatives has shown fast and selective Pictet–Spengler reactions with aldehyde-containing biomolecules.[50] Under conditions of 10 mM cyclic imine **1** with 1 mM 1*H*-pyrrole-1-propionate (as a soluble pyrrole-Lys mimic), we determined a second order rate constant of 5.9 × 10^{-2} $M^{-1}s^{-1}$ (Figure 1, Figure S2). This ~200-fold increase relative to Tyr suggests cyclic imines may be effective reactive groups for proteomic profiling of lysine pyrrolation.

Stability and reversibility of cyclic imines with tyrosine and cysteine. To validate the stability of cyclic imines as covalent warheads, imines **1-4** were evaluated by LC/MS after 96-hour incubation in PBS, 0.1M HCl, and 0.1M NaOH (Table S1). Compounds **1** and **4** were stable under all conditions. Both ester containing compounds **2** and **3** hydrolyzed under basic conditions. Aromatic ester imine **3** was unstable in PBS, with a mixture of hydrolysis and Mannich reaction with the hydrolysis product 2-amino phenol. We also evaluated the stability of the product of imine **1** with Ac-Tyr-NHMe in 0.13 M (1%) TFA, 0.53 M (1%) NaOH, or PBS buffer for 96 hours and observed only marginal decomposition of the Tyr Mannich product (Figure S4).

Thiol addition to the imine is reversible,[38,43] yet this reaction may limit the desired reactivity of imines to tyrosines in cellular contexts where glutathione concentrations can be 1-10 mM.[51,52] To evaluate this reversibility, the pre-formed thioaminal product of **1** with N-acetyl-cysteine methyl amide was treated with either glutathione (1 M) or Ac-Tyr-NHMe (100 mM). Both glutathione and Ac-Tyr-NHMe outcompeted the cysteine product after 24 hours (Figure S5). To evaluate potential effects of cellular thiols on tyrosine labeling rate, the cyclic imine-Tyr reaction (at 5 mM and 100 mM, respectively) was evaluated over time in the presence of cysteine (5 mM) (Figure S6). The presence of cysteine slightly slowed the reaction rate of tyrosine-imine compared to the control.

Covalent labeling of cyclic imine with tyrosine-containing peptide (Angiotensin II) and protein (CBX8 chromodomain). To confirm reactivity and selectivity within a peptide context, imine **1** (50 mM) was incubated with the tyrosine-containing 8-mer peptide angiotensin II (DRVYIHPF) (10 mM) (Figure S7). The combined yield of mono-labeled and di-labeled angiotensin II was ~ 45% as quantified by LC/MS. Imine **1** was also incubated with a small protein (recombinant CBX8 chromodomain (ChD)), which contains multiple tyrosines and tryptophans. With overnight incubation, two to three additions of the imine were observed by mass spectrometry (Figure S8).

Design and synthesis of cyclic imine-containing CBX8 ChD inhibitors. SW2_110A is a selective CBX8 ChD inhibitor with an 800 nM K_d (Figure 2C).[53,54] Although **SW2_110A** demonstrates high selectivity for CBX8 over CBX4, CBX6, and CBX7, it is only 6-fold selective over CBX2. We used amino acid sequence alignment and an X-ray crystal structure of a similar ligand (**UNC3866**) bound to CBX8 (Figure 3B),[55] to identify a tyrosine (Y39) residue adjacent the diethyllysine binding site that is a histidine in CBX2. One of the ethyl groups of the alkylated lysine side chain of the ligand is solvent exposed and points in the direction of Y39 on CBX8, which is ~8-9 Å from the lysine nitrogen (Figure 2B). Thus, we synthesized several potential covalent ligands by linking warheads off this ethyl group of **SW2_110A**. (Figure 2C).

The analogs were synthesized using standard, solid phase peptide synthesis of **SW2_110A** with a nosyl-protected lysine (Schemes S7-S13), which was further elaborated on-resin by alkylation with an alkylhalide or Fukuyama-Mitsunobu chemistry.[56] Due to concerns about imine stability throughout synthesis, we prepared the warhead as a primary amine suitably placed adjacent to a serine amide or ester as a latent electrophile. After purification, the compounds were treated *in situ* with sodium periodate to oxidize the 1,2-amino alcohol of the serine to

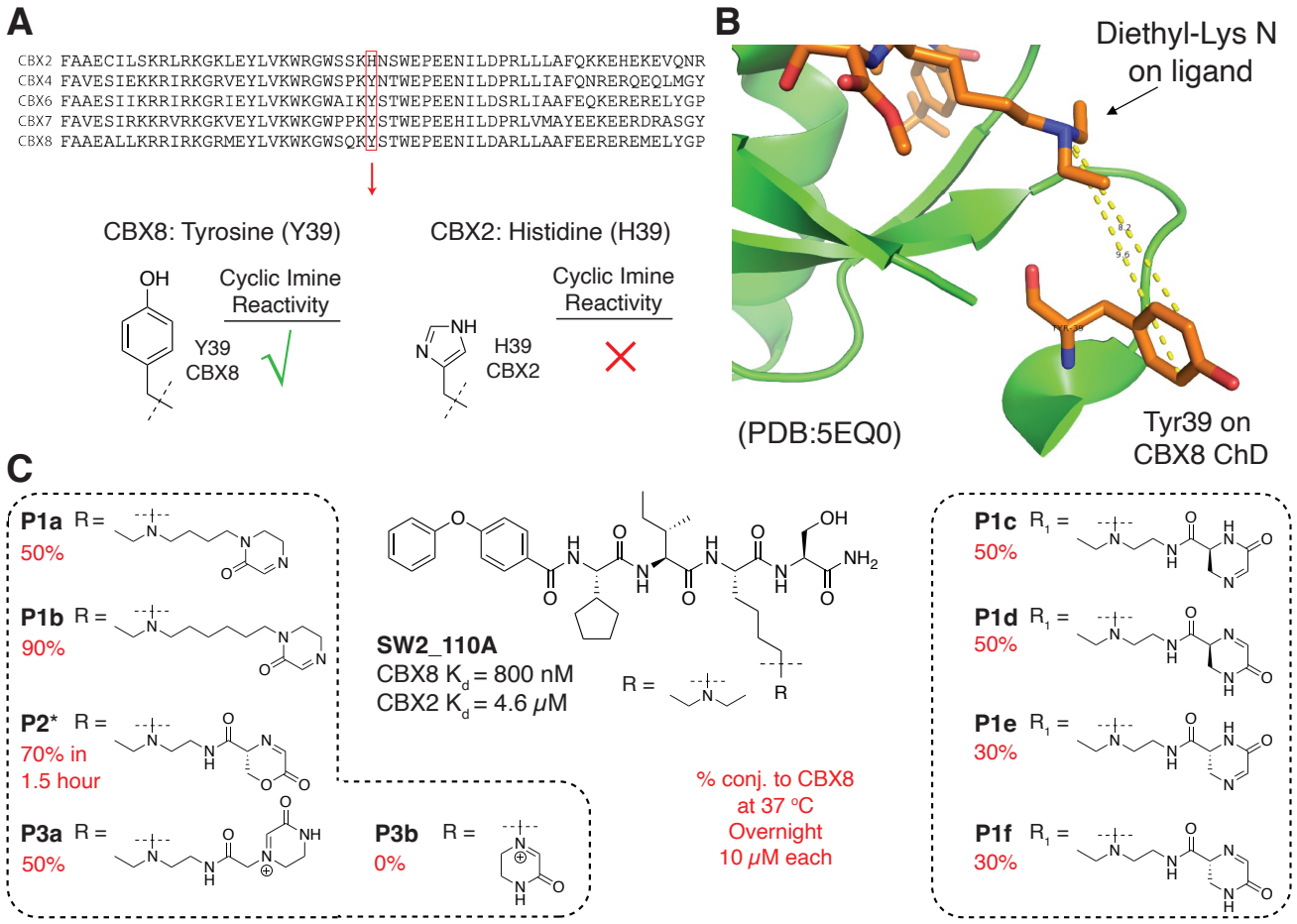

Figure 2. Design of covalent inhibitors to the CBX8 chromodomain (ChD). (A) Sequence alignment of the five CBX ChDs in the Polycomb repressive complex I shows a histidine in CBX2 at position 39 that allows the reactivity of the tyrosine in CBX8 to be exploited for improved inhibitor specificity. (B) Crystal structure of peptide ligand UNC3866 bound to CBX8 Chd (PDB code 5EQ0) with Tyr39 adjacent to the diethyllysine group. (C) Synthesized derivatives of SW2_110A containing cyclic imine or iminium warheads. Percent covalent conjugation was determined by UV integration on LC/MS after overnight incubation at 10 μM compound and protein at 37 °C.

produce an alpha-aldehyde amide/ester, which then spontaneously cyclized to give the desired imines.

To rule out concerns that the phenoxyphenyl moiety of **SW2_110A** may self-react with the warhead, we performed a 24-hour incubation of **P1b** in PBS followed by treatment with sodium cyanoborohydride (10 eq.). Mass spectrometry indicated full conversion of imine to amine (Figure S9). Similarly, we tested the longer-term stability of **P1b** in acidic (100 mM HCl), basic (100 mM NaOH), and neutral PBS buffers and observed no significant degradation after 96 h at room temperature.

Covalent labeling of cyclic imine containing ligands to CBX8 ChD. To evaluate the reaction with CBX8 ChD, all cyclic imine ligands were tested with purified CBX8 ChD. To saturate the binding of inhibitor to protein, 10 μM of the covalent inhibitors were incubated with 10 μM CBX8 ChD (~10-fold over the K_d) in PBS buffer at 37 °C for 12 hours. The labeling of inhibitors to CBX8 ChD was quantified by LC/MS (Figure 2C, 4A & B, and Figure S10-12). Among the cyclic amide imine series (**P1's**), compound **P1a**, with a 6-carbon linker, gave the best yield for labeling the CBX8 ChD (~90 %). This compound was also tested in the presence of 10 mM GSH, and no effect on yield was observed (Figure S13). Due to the enhanced reactivity of iminolactone (warhead **2**), CBX8 ChD labeling using ester imine inhibitor **P2** was considerably faster and around 70% protein labeling was achieved in 1.5 hour (Figure 2A,B, Figure S12). We additionally prepared two iminium warhead compounds, **P3a** and **P3b**. Despite the low intrinsic reactivity observed with model iminium **3** and Tyr (Table 1), inhibitor **P3a** gave a labeling yield (50%) that was comparable to the more reactive iminolactams. This may suggest assistance in the reaction from the local environment on the protein.

Time-dependent fluorescence displacement assay. We used a fluorescence polarization (FP) displacement assay to evaluate the covalent binding of cyclic imine warhead containing inhibitors. Without additional incubation time, the non-covalent inhibitor **SW2_110A** and optimal covalent inhibitors **P1b** (iminolactam) and **P2** (iminolactone) have comparable IC_{50} values (Figures S14-15), which suggests that the structural modification of the warhead does not significantly change the affinity. With further incubation, **P1b** and **P2** displayed a time-dependent increase of potency (decrease of IC_{50}), while non-covalent inhibitor **SW2_110A** did not (Figure 4C & Figures S14-15).

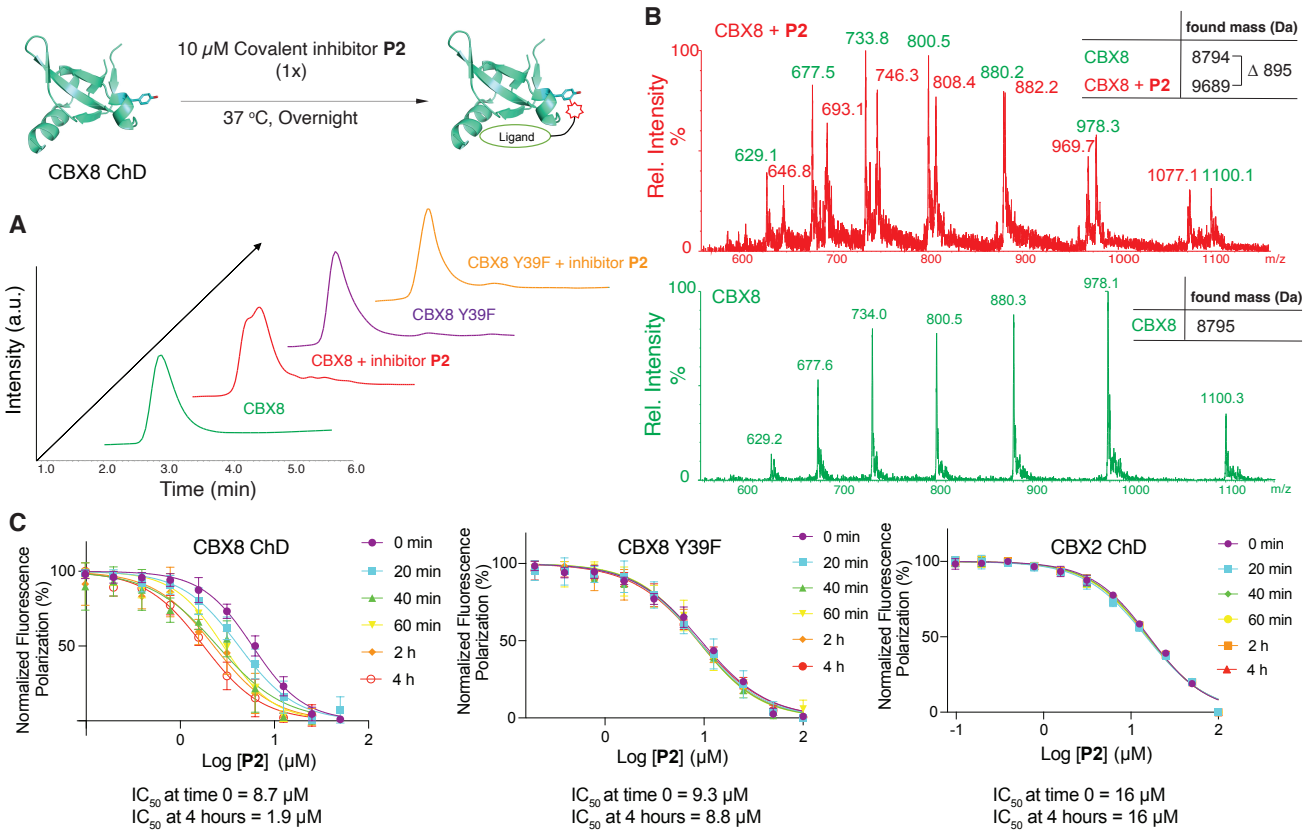

Figure 3. Characterization of ligand directed protein labeling with iminolactone inhibitor **P2**. (A) The fraction of labeled protein as determined by UV integration on reverse phase HPLC. CBX8 ChD and **P2** were incubated at 10 μM each for 16 hours at 37 °C. UV absorption measured at 215 nm. (B) Mass spectra of CBX8 ChD treated overnight with inhibitor **P2** (top, red) and control CBX8 ChD (bottom, green). Observed masses are shown (expected average mass for CBX8 ChD = 8792 Da). The observed mass difference (895 Da) corresponds to the expected mass change of 901 Da. (C) Time dependent fluorescence polarization displacement assays of indicated chromodomains with **P2**. Assays were conducted using **SW2_123** as an FP probe (Figure S15) at 100 nM. All proteins were used at 2 μM in PBS (pH 7), 0.02% Tween 20. Error bars represent s.d.

To validate protein stability over the incubation time of the assay, the K_d of the FP probe (**SW2_123**) was measured at time 0 and 20 hours and determined to be unchanged, indicating good stability (Figure S16).

Validation of CBX8 Labeling at Y39. To validate labeling of the targeted tyrosine residue (Y39), this amino acid was mutated to phenylalanine (Figure S17), which is structurally similar but lacks reactivity to the cyclic imine. The fluorescence displacement assay indicated inhibitors bind to wild type or mutant CBX8 (Y39F) with comparable IC_{50} values (9.3 μM versus 8.7 μM for **P2**, 7.4 μM versus 7.3 μM for **P1b**, respectively) (Figure 3C, Figure S14); however, both the time-dependent FP assay (Figure 3C) and MS protein labeling experiments (Figure 3A, Figure S18) indicate that covalent inhibitors fail to label the mutant CBX8 Y39F. Similarly, for CBX2 ChD, no change in apparent affinity was observed over time in the FP assay (Figure 3C & Figure S15), and no labeled protein was detected by MS. Together these results support the ligand-directed labeling of Y39 on CBX8.

Proteomic Selectivity of Cyclic Imine Inhibitor. To demonstrate the covalent labeling of endogenous CBX8, in-gel fluorescence labeling was performed (Figure 4A,B). After incubation of the inhibitor **P2** at 1 μM in HEK293T cell lysates for 1h at 37 °C, click chemistry was conducted to conjugate TAMRA-azide to the C-terminal alkyne of **P2** prior to SDS-PAGE. Gel analysis showed a prominent fluorescent band, which is approximately the molecular weight of CBX8. With co-incubation of excess non-covalent inhibitor **SW2_110A** (~20 μM, 20 eq), protein labeling was reduced (Figure 4A). We additionally demonstrated the dose-dependency of labeling of CBX8 with the covalent inhibitor from 10 nM to 1000 nM inhibitor concentration (Figure 4B).

To corroborate that imine inhibitors can covalently capture the endogenous, full length CBX8, pulldown assays were also performed making use of propargyl amide modified inhibitors and click chemistry to biotin-azide (Figure 4 C,D). Besides **P2**, we prepared a propargyl amide derivative of 6-carbon linker iminolactam inhibitor, **P1bP** (Scheme S5). Covalent inhibitors **P2**, **P1bP**, and a non-covalent inhibitor **SW2_110A** were incubated with 293T cell lysates at 1 μM for protein labeling. For competition, an excess (10-100 eq) of the non-covalent inhibitor was added. Labeled lysates were then clicked to a biotin-azide for affinity purification. Under non-denaturing washing buffer conditions, both covalent and non-covalent inhibitors enriched CBX8 from lysates (Figure 4C). Using more stringent washing conditions, only covalent inhibitor **P2** enriched CBX8 from lysates (Figure 4C). To remove non-specific background from highly expressed CBX7, and the

abundant nuclear protein BRG1, we used fully denaturing washing conditions of 0.2-1% SDS in PBS (Figure 4C,D) or 6M urea (Figure S19).[57,58] Under these conditions, CBX8 was still captured by the covalent inhibitor, while other CBXs, known CBX8 interacting protein RING1B, or non-specific protein BRG1 were not. To further demonstrate ligand-dependent covalent labeling, an excess of the non-covalent inhibitor was doped in for competition. With 100 equivalents of competing ligand added, covalent labeling of CBX8 by either compound **P2** or **P1bP** was reduced, as quantitated by western blot (Figure 4D).

Cellular activity of covalent inhibitors in MLL-AF9 transformed leukemia cell line. We next assessed if imine inhibitors have improved cellular activity using a disease-relevant cell model. We previously reported that the non-covalent inhibitor **SW2_110A** inhibits CBX8 binding to chromatin and reduces CBX8-mediated gene expression in MLL-AF9 transformed leukemia.[53] Using this same model, we compared the covalent inhibitors with non-covalent inhibitor **SW2_110A** in THP1 cell lines. Initially, **P1** series inhibitors and **P3a** were tested at 10 μM for reducing the gene expression of *HOXA9*, a known target of

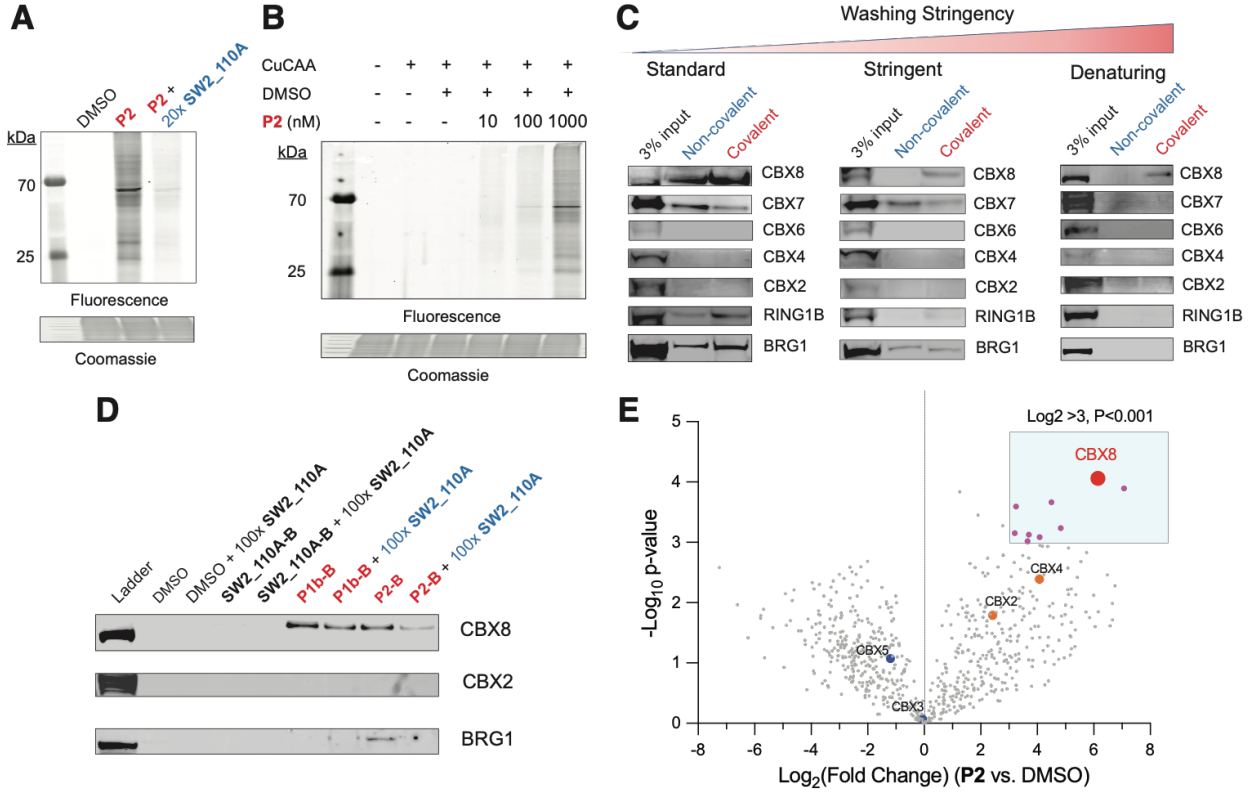

Figure 4. Proteomic activity of covalent inhibitors for CBX8**.** (A) SDS-PAGE, in-gel fluorescence analysis of HEK293T lysates treated with **P2** (1 μM) and Cu-catalyzed azide-alkyne cycloaddition (CuCAA) to azide-TAMRA (B) Additional SDS-PAGE, fluorescence analysis of HEK293T lysates as in (A) with **P2** at 10, 100, and 1000 nM concentrations. (C) Chemoprecipitations from HEK293T cell lysates using biotin-labeled **SW2_110A** (**SW2_110A-B**) and biotin-labeled **P2** (**P2-B**) were performed with various washing conditions and analyzed for protein enrichment by immunoblot. Standard wash: 50 mM Tris-HCl, 150 mM NaCl, 0.3% NP-40. Stringent wash: Modified RIPA buffer: 50 mM Tris-HCl, 150 mM NaCl, 1 mM EDTA, 1% NP-40, 0.1% DOC. Denaturing wash: 0.2-1% SDS gradient in PBS. RING1B is a subunit of PRC1 with the CBX proteins. BRG1 is non-associated nuclear protein included as control for non-specific binding (D) Immunoblot analysis of chemoprecipitations from HEK293T cell lysates with biotin-labeled **P1b** (**P1b-B**) and **P2-B** in the presence or absence of competing ligand **SW2_110A**. Stringent wash conditions were applied as in (C). (E) Volcano plot of streptavidin enrichment for proteins identified in **P2-B** treated 293T lysates versus a DMSO control. N = 2, biological replicates; P is the Benjamini-Hochberg adjusted P value.

To evaluate and quantitate covalent ligand activity in whole cell proteomes, mass spectrometry analysis was performed after compound pulldown (chemoIP-MS) (Figure 4E). CBX8 was robustly enriched using the biotinylated, covalent inhibitor **P2-B**. Of the nine proteins significantly enriched with **P2-B** ($\log_2$(**P2-B**/DMSO) > 3, P < 0.001), only CBX8 enrichment was significantly reduced with competing non-reactive ligand **SW2_110A**, indicating ligand-dependent, covalent labeling of endogenous CBX8 from lysates (Figure S20). Results were similar using iminolactam inhibitor **P1bP**, (Figure S20).

CBX8. The covalent inhibitors (**P1a-f)** and **P3a** reduced expression to a greater extent than the non-covalent inhibitor (Figure S21). Consistent with it having the greatest in vitro reactivity among those tested, inhibitor **P1b** was the most effective at reducing *HOXA9* gene expression where 10 μM **P1b** treatment reduced gene expression to a similar extent as 100 μM **SW2_110A** (Figure 5A). We subsequently tested the two optimal inhibitors **P1bP** and **P2** for dose-dependency in this cellular assay. Dose curves indicate that these covalent inhibitors have 30 to 100-fold improvement of cellular activity compared to the non-covalent inhibitor (Figure 5B).

CONCLUSION

We report the development of a novel cyclic imine warheads and the first demonstration of ligand directed Mannich chemistry for tyrosine conjugation. We performed quantitative evaluation of the second order reaction rates of cyclic imines to tyrosine. We designed and tested a series of imine warheads and developed an ester cyclic imine (iminolactone **2**) as the optimally reactive and efficient warhead for tyrosine labeling with a second order rate constant of 2.9 $\times 10^{-3}$ M^{-1} s^{-1} at 37 °C. In addition, we showed the reactivity of imine **1** towards tryptophan and pyrrolated lysine (2-ethyl pyrrole), implicating potential broader bioconjugation and chemical probe applications. Importantly, these warheads showed excellent stability in aqueous solutions, which is a major limitation for current Tyr modification chemistries.

We synthesized derivatives of a previously developed CBX8 chromodomain inhibitor **SW2_110A** containing warhead imines **1**, **2**, and **3**. MS characterization confirmed covalent conjugation to the target protein. Biochemical assays further confirmed reactivity specifically at Tyr39 of CBX8 and demonstrated selective targeting of CBX8 over CBX2. This selectivity was further validated with chemoprecipitations of endogenous proteins using biotinylated inhibitors. Furthermore, proteomic MS analysis indicated excellent target engagement with the covalent inhibitors in a whole cell proteome with CBX8 being among the most highly enriched proteins. Lastly, these covalent inhibitors showed significant improvements in cellular activity.

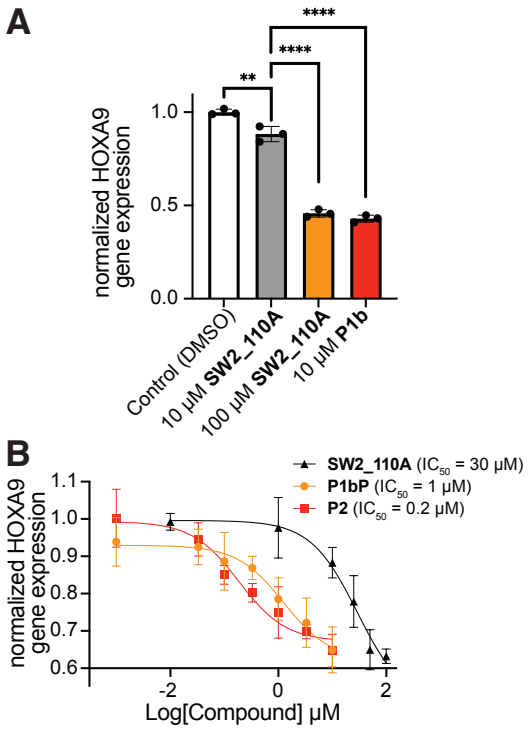

Figure 5. Cellular activity of covalent, cyclic imine inhibitors to CBX8. (A) qRT-PCR analysis of *HOXA9* gene expression in THP1 cells after 48 h of compound treatment at the indicated dose. N= 3. Error bars represent s.d. Statistical significance calculated using student's t-test. ** = $p < 0.01$, **** = $p < 0.0001$, (B) qRT-PCR analysis of *HOXA9* gene expression in THP1 cells treated with increasing doses of compound for 48 h. N = 3. Error bars represent s.d.

Further improvement of warhead properties, such as tuning imine reactivity with additional substitution, are anticipated future directions. Proteomic studies for discovery of ligandable tyrosines or druggable target identification would also be potential applications for this Mannich-type electrophile. Given the limitations of current chemistry for tyrosine modification, this chemistry should find several uses in medicinal chemistry and bioconjugation.

ASSOCIATED CONTENT

Supporting Information

The Supporting Information is available free of charge on the ACS Publications website.
Supporting Information Figures S1-S21, Supporting Information Table 1, Supporting Schemes S1-S13, experimental procedures and compound characterization data (PDF)

AUTHOR INFORMATION

Corresponding Author

* Casey J. Krusemark - Department of Medicinal Chemistry and Molecular Pharmacology, Purdue Center for Cancer Research, Purdue University, West Lafayette, Indiana 47907, United States; ORCID: 0000-0003-2964-3520; Email: cjk@purdue.edu

Author Contributions

C.J.K. conceptualized the project. S.W., E.C.D., and C.J.K. designed experiments. S.W. synthesized molecules and performed all *in vitro* and cellular assays. M.H. and W.A.T. performed and analyzed MS proteomics experiments. S.W. and C.J.K. wrote the manuscript with assistance from E.C.D. All authors have given approval to the final version of the manuscript.

Funding Sources

CJK is supported by NIH, R35GM128894, ECD is supported by ACS, RSG-21-012-01-DMC, WAT is supported by NIH, 1RF1AG064250, Purdue Center for Cancer Research NIH grant P30 CA023168

Notes

The authors declare no competing financial interest.

ACKNOWLEDGMENT

We thank past lab members Dr. Fei Tang for compound **5** synthesis and Corey Boese for initial optimization of Fukuyama-Mitsunobu chemistry on solid phase. We thank Dr. Amol Mhetre and Dr. Mingji Dai for helpful discussions.

REFERENCES

(1) Gehringer, M.; Laufer, S. A. Emerging and Re-Emerging Warheads for Targeted Covalent Inhibitors: Applications in Medicinal Chemistry and Chemical Biology. *J. Med. Chem.* **2019**, *62* (12), 5673–5724.

(2) Baillie, T. A. Targeted Covalent Inhibitors for Drug Design. *Angew. Chemie Int. Ed.* **2016**, *55* (43), 13408–13421.

(3) Ghosh, A. K.; Samanta, I.; Mondal, A.; Liu, W. R. Covalent Inhibition in Drug Discovery. *ChemMedChem* **2019**, *14* (9), 889–906.

(4) Ueda, T.; Tamura, T.; Kawano, M.; Shiono, K.; Hobor, F.;

Wilson, A. J.; Hamachi, I. Enhanced Suppression of a Protein-Protein Interaction in Cells Using Small-Molecule Covalent Inhibitors Based on an N-Acyl- N-Alkyl Sulfonamide Warhead. *J. Am. Chem. Soc.* **2021**, *143* (12), 4766–4774.

(5) Way, J. C. Covalent Modification as a Strategy to Block Protein–Protein Interactions with Small-Molecule Drugs. *Curr. Opin. Chem. Biol.* **2000**, *4* (1), 40–46.

(6) Deak, P. E.; Kim, B.; Qayum, A. A.; Shin, J.; Vitalpur, G.; Kloepfer, K. M.; Turner, M. J.; Smith, N.; Shreffler, W. G.; Kiziltepe, T.; Kaplan, M. H.; Bilgicer, B. Designer Covalent Heterobivalent Inhibitors Prevent IgE-Dependent Responses to Peanut Allergen. *Proc. Natl. Acad. Sci. U. S. A.* **2019**, *116* (18), 8966–8974.

(7) Bum-Erdene, K.; Zhou, D.; Gonzalez-Gutierrez, G.; Ghozayel, M. K.; Si, Y.; Xu, D.; Shannon, H. E.; Bailey, B. J.; Corson, T. W.; Pollok, K. E.; Wells, C. D.; Meroueh, S. O. Small-Molecule Covalent Modification of Conserved Cysteine Leads to Allosteric Inhibition of the TEAD·Yap Protein-Protein Interaction. *Cell Chem. Biol.* **2019**, *26* (3), 378-389.e13.

(8) He, H.; Jiang, H.; Chen, Y.; Ye, J.; Wang, A.; Wang, C.; Liu, Q.; Liang, G.; Deng, X.; Jiang, W.; Zhou, R. Oridonin Is a Covalent NLRP3 Inhibitor with Strong Anti-Inflammasome Activity. *Nat. Commun. 2018 91* **2018**, *9* (1), 1–12.

(9) Lv, Z.; Yuan, L.; Atkison, J. H.; Williams, K. M.; Vega, R.; Sessions, E. H.; Divlianska, D. B.; Davies, C.; Chen, Y.; Olsen, S. K. Molecular Mechanism of a Covalent Allosteric Inhibitor of SUMO E1 Activating Enzyme. *Nat. Commun. 2018 91* **2018**, *9* (1), 1–12.

(10) Zeng, M.; Lu, J.; Li, L.; Feru, F.; Quan, C.; Gero, T. W.; Ficarro, S. B.; Xiong, Y.; Ambrogio, C.; Paranal, R. M.; Catalano, M.; Shao, J.; Wong, K. K.; Marto, J. A.; Fischer, E. S.; Jänne, P. A.; Scott, D. A.; Westover, K. D.; Gray, N. S. Potent and Selective Covalent Quinazoline Inhibitors of KRAS G12C. *Cell Chem. Biol.* **2017**, *24* (8), 1005-1016.e3.

(11) Ishiba, H.; Noguchi, T.; Shu, K.; Ohno, H.; Honda, K.; Kondoh, Y.; Osada, H.; Fujii, N.; Oishi, S. Investigation of the Inhibitory Mechanism of Apomorphine against MDM2–P53 Interaction. *Bioorg. Med. Chem. Lett.* **2017**, *27* (11), 2571–2574.

(12) Yu, Y.; Nie, Y.; Feng, Q.; Qu, J.; Wang, R.; Bian, L.; Xia, J. Targeted Covalent Inhibition of Grb2-Sos1 Interaction through Proximity-Induced Conjugation in Breast Cancer Cells. *Mol. Pharm.* **2017**, *14* (5), 1548–1557.

(13) Akçay, G.; Belmonte, M. A.; Aquila, B.; Chuaqui, C.; Hird, A. W.; Lamb, M. L.; Rawlins, P. B.; Su, N.; Tentarelli, S.; Grimster, N. P.; Su, Q. Inhibition of Mcl-1 through Covalent Modification of a Noncatalytic Lysine Side Chain. *Nat. Chem. Biol.* **2016**, *12* (11), 931–936.

(14) Cardoso, R.; Love, R.; Nilsson, C. L.; Bergqvist, S.; Nowlin, D.; Yan, J.; Liu, K. K. C.; Zhu, J.; Chen, P.; Deng, Y. L.; Dyson, H. J.; Greig, M. J.; Brooun, A. Identification of Cys255 in HIF-1α as a Novel Site for Development of Covalent Inhibitors of HIF-1α/ARNT PasB Domain Protein–Protein Interaction. *Protein Sci.* **2012**, *21* (12), 1885–1896.

(15) Arkin, M. R.; Tang, Y.; Wells, J. A. Small-Molecule Inhibitors of Protein-Protein Interactions: Progressing toward the Reality. *Chem. Biol.* **2014**, *21* (9), 1102–1114.

(16) Cheng, S. S.; Yang, G. J.; Wang, W.; Leung, C. H.; Ma, D. L. The Design and Development of Covalent Protein-Protein Interaction Inhibitors for Cancer Treatment. *J. Hematol. Oncol.* **2020**, *13* (1), 1–14.

(17) Abbasov, M. E.; Kavanagh, M. E.; Ichu, T. A.; Lazear, M. R.; Tao, Y.; Crowley, V. M.; am Ende, C. W.; Hacker, S. M.; Ho, J.; Dix, M. M.; Suciu, R.; Hayward, M. M.; Kiessling, L. L.; Cravatt, B. F. A Proteome-Wide Atlas of Lysine-Reactive Chemistry. *Nat. Chem. 2021 1311* **2021**, *13* (11), 1081–1092.

(18) Mukherjee, H.; Grimster, N. P. Beyond Cysteine: Recent Developments in the Area of Targeted Covalent Inhibition. *Curr. Opin. Chem. Biol.* **2018**, *44*, 30–38.

(19) Koide, S.; Sidhu, S. S. The Importance of Being Tyrosine: Lessons in Molecular Recognition from Minimalist Synthetic Binding Proteins. *ACS Chem. Biol.* **2009**, *4* (5), 325–334.

(20) Hett, E. C.; Xu, H.; Geoghegan, K. F.; Gopalsamy, A.; Kyne, R. E.; Menard, C. A.; Narayanan, A.; Parikh, M. D.; Liu, S.; Roberts, L.; Robinson, R. P.; Tones, M. A.; Jones, L. H. Rational Targeting of Active-Site Tyrosine Residues Using Sulfonyl Fluoride Probes. *ACS Chem. Biol.* **2015**, *10* (4), 1094–1098.

(21) Gambini, L.; Baggio, C.; Udompholkul, P.; Jossart, J.; Salem, A. F.; Perry, J. J. P.; Pellecchia, M. Covalent Inhibitors of Protein-Protein Interactions Targeting Lysine, Tyrosine, or Histidine Residues. *J. Med. Chem.* **2019**, *62* (11), 5616–5627.

(22) Bartesaghi, S.; Ferrer-Sueta, G.; Peluffo, G.; Valez, V.; Zhang, H.; Kalyanaraman, B.; Radi, R. Protein Tyrosine Nitration in Hydrophilic and Hydrophobic Environments. *Amino Acids* **2007**, *32* (4), 501–515.

(23) Pawson, T.; Nash, P. Assembly of Cell Regulatory Systems through Protein Interaction Domains. *Science (80-.).* **2003**, *300* (5618), 445–452.

(24) Scrutton, N. S.; Raine, A. R. C. Cation-π Bonding and Amino-Aromatic Interactions in the Biomolecular Recognition of Substituted Ammonium Ligands. *Biochem. J* **1996**, *319*, 1–8.

(25) Santiago, C.; Nguyen, K.; Schapira, M. Druggability of Methyl-Lysine Binding Sites. *J. Comput. Aided. Mol. Des.* **2011**, *25* (12), 1171–1178.

(26) Bowkett, D.; Talon, R.; Tallant, C.; Schofield, C.; von Delft, F.; Knapp, S.; Bruton, G.; Brennan, P. E. Identifying Small-Molecule Binding Sites for Epigenetic Proteins at Domain–Domain Interfaces. *ChemMedChem* **2018**, *13* (10), 1051.

(27) Narayanan, A.; Jones, L. H. Sulfonyl Fluorides as Privileged Warheads in Chemical Biology. *Chem. Sci.* **2015**, *6* (5), 2650–2659.

(28) Lonsdale, R.; Ward, R. A. Structure-Based Design of Targeted Covalent Inhibitors. *Chem. Soc. Rev.* **2018**, *47* (11), 3816–3830.

(29) Dong, J.; Krasnova, L.; Finn, M. G.; Barry Sharpless, K. Sulfur(VI) Fluoride Exchange (SuFEx): Another Good Reaction for Click Chemistry. *Angew. Chemie Int. Ed.* **2014**, *53* (36), 9430–9448.

(30) Zhou, H.; Mukherjee, P.; Liu, R.; Evrard, E.; Wang, D.; Humphrey, J. M.; Butler, T. W.; Hoth, L. R.; Sperry, J. B.; Sakata, S. K.; Helal, C. J.; Am Ende, C. W. Introduction of a Crystalline, Shelf-Stable Reagent for the Synthesis of Sulfur(VI) Fluorides. *Org. Lett.* **2018**, *20* (3), 812–815.

(31) Martín-Gago, P.; Olsen, C. A. Arylfluorosulfate-Based Electrophiles for Covalent Protein Labeling: A New Addition to the Arsenal. *Angew. Chemie Int. Ed.* **2019**, *58* (4), 957–966.

(32) Decoene, K. W.; Unal, K.; Staes, A.; Gevaert, K.; Winne, J. M.; Madder, A. Protein Conjugation with Triazolinediones: Switching from a General Tyrosine-Selective Labeling Method to a Highly Specific Tryptophan Bioconjugation Strategy. **2021**.

(33) Ban, H.; Nagano, M.; Gavrilyuk, J.; Hakamata, W.; Inokuma, T.; Barbas, C. F. Facile and Stabile Linkages through Tyrosine: Bioconjugation Strategies with the Tyrosine-Click Reaction. *Bioconjug. Chem.* **2013**, *24* (4), 520–532.

(34) Schlick, T. L.; Ding, Z.; Kovacs, E. W.; Francis, M. B. Dual-Surface Modification of the Tobacco Mosaic Virus. *J. Am. Chem. Soc.* **2005**, *127* (11), 3718–3723.

(35) Hooker, J. M.; Kovacs, E. W.; Francis, M. B. Interior Surface Modification of Bacteriophage MS2. *J. Am. Chem. Soc.* **2004**, *126* (12), 3718–3719.

(36) Sengupta, S.; Chandrasekaran, S. Modifications of Amino Acids Using Arenediazonium Salts. *Org. Biomol. Chem.* **2019**, *17* (36), 8308–8329.

(37) Mannich, C.; Krösche, W. Ueber Ein Kondensationsprodukt Aus Formaldehyd, Ammoniak Und Antipyrin. *Arch. Pharm. (Weinheim).* **1912**, *250* (1), 647–667.

(38) Minakawa, M.; Guo, H. M.; Tanaka, F. Imines That React with Phenols in Water over a Wide PH Range. *J. Org. Chem.* **2008**, *73* (21), 8669–8672.

(39) Lonsdale, R.; Burgess, J.; Colclough, N.; Davies, N. L.; Lenz, E. M.; Orton, A. L.; Ward, R. A. Expanding the

Armory: Predicting and Tuning Covalent Warhead Reactivity. *J. Chem. Inf. Model.* **2017**, *57* (12), 3124–3137.
(40) Cummings, T. F.; Shelton, J. R. Mannich Reaction Mechanisms. *J. Org. Chem.* **1960**, *25* (3), 419–423.
(41) Sim, Y. E.; Nwajiobi, O.; Mahesh, S.; Cohen, R. D.; Reibarkh, M. Y.; Raj, M. Secondary Amine Selective Petasis (SASP) Bioconjugation. *Chem. Sci.* **2020**, *11* (1), 53–61.
(42) Eldin, S.; Jencks, W. P. Lifetimes of Iminium Ions in Aqueous Solution. *J. Am. Chem. Soc.* **1995**, *117* (17), 4851–4857.
(43) Cavaca, L. A. S.; Gomes, R. F. A.; Afonso, C. A. M. Preparation of Thioaminals in Water. *Mol. 2022, Vol. 27, Page 1673* **2022**, *27* (5), 1673.
(44) McFarland, J. M.; Joshi, N. S.; Francis, M. B. Characterization of a Three-Component Coupling Reaction on Proteins by Isotopic Labeling and Nuclear Magnetic Resonance Spectroscopy. *J. Am. Chem. Soc.* **2008**, *130* (24), 7639–7644.
(45) Antos, J. M.; Francis, M. B. Selective Tryptophan Modification with Rhodium Carbenoids in Aqueous Solution. *J. Am. Chem. Soc.* **2004**, *126* (33), 10256–10257.
(46) Larda, S. T.; Pichugin, D.; Prosser, R. S. Site-Specific Labeling of Protein Lysine Residues and N-Terminal Amino Groups with Indoles and Indole-Derivatives. *Bioconjug. Chem.* **2015**, *26* (12), 2376–2383.
(47) Minakawa, M.; Guo, H. M.; Tanaka, F. Imines That React with Phenols in Water over a Wide PH Range. *J. Org. Chem.* **2008**, *73* (21), 8669–8672.
(48) Miyashita, H.; Chikazawa, M.; Otaki, N.; Hioki, Y.; Shimozu, Y.; Nakashima, F.; Shibata, T.; Hagihara, Y.; Maruyama, S.; Matsumi, N.; Uchida, K. Lysine Pyrrolation Is a Naturally-Occurring Covalent Modification Involved in the Production of DNA Mimic Proteins. **2014**.
(49) Chikazawa, M.; Yoshitake, J.; Lim, S. Y.; Iwata, S.; Negishi, L.; Shibata, T.; Uchida, K. Glycolaldehyde Is an Endogenous Source of Lysine N-Pyrrolation. *J. Biol. Chem.* **2020**, *295* (22), 7697–7709.
(50) Pomplun, S.; Mohamed, M. Y. H.; Oelschlaegel, T.; Wellner, C.; Bergmann, F. Efficient Pictet–Spengler Bioconjugation with N-Substituted Pyrrolyl Alanine Derivatives. *Angew. Chemie - Int. Ed.* **2019**, *58* (11), 3542–3547.
(51) Meister, A. Glutathione Metabolism and Its Selective Modification. *J. Biol. Chem.* **1988**, *263* (33), 17205–17208.
(52) Forman, H. J.; Zhang, H.; Rinna, A. Glutathione: Overview of Its Protective Roles, Measurement, and Biosynthesis. *Mol. Aspects Med.* **2009**, *30* (1–2), 1.
(53) Wang, S.; Denton, K. E.; Hobbs, K. F.; Weaver, T.; McFarlane, J. M. B.; Connelly, K. E.; Gignac, M. C.; Milosevich, N.; Hof, F.; Paci, I.; Musselman, C. A.; Dykhuizen, E. C.; Krusemark, C. J. Optimization of Ligands Using Focused DNA-Encoded Libraries to Develop a Selective, Cell-Permeable CBX8 Chromodomain Inhibitor. *ACS Chem. Biol.* **2020**, *15* (1).
(54) Denton, K. E.; Wang, S.; Gignac, M. C.; Milosevich, N.; Hof, F.; Dykhuizen, E. C.; Krusemark, C. J. Robustness of In Vitro Selection Assays of DNA-Encoded Peptidomimetic Ligands to CBX7 and CBX8. *SLAS Discov.* **2018**.
(55) Stuckey, J. I.; Dickson, B. M.; Cheng, N.; Liu, Y.; Norris, J. L.; Cholensky, S. H.; Tempel, W.; Qin, S.; Huber, K. G.; Sagum, C.; Black, K.; Li, F.; Huang, X.-P.; Roth, B. L.; Baughman, B. M.; Senisterra, G.; Pattenden, S. G.; Vedadi, M.; Brown, P. J.; Bedford, M. T.; Min, J.; Arrowsmith, C. H.; James, L. I.; Frye, S. V. A Cellular Chemical Probe Targeting the Chromodomains of Polycomb Repressive Complex 1. *Nat. Chem. Biol.* **2016**, *12* (3), 180–187.
(56) Kan, T.; Fukuyama, T. Ns Strategies: A Highly Versatile Synthetic Method for Amines. *Chem. Commun.* **2004**, *0* (4), 353–359.
(57) Weerapana, E.; Speers, A. E.; Cravatt, B. F. Tandem Orthogonal Proteolysis-Activity-Based Protein Profiling (TOP-ABPP)-a General Method for Mapping Sites of Probe Modification in Proteomes. **2007**.
(58) Kurzban, G. P.; Bayer, E. A.; Wilchek, M.; Horowitz, P. M. The Quaternary Structure of Streptavidin in Urea. *J. Biol. Chem.* **1991**, *266* (22), 14470–14477.